

Computational drug repurposing: Posaconazole emerges as a potent NAMPT inhibitor, offering promise for precision cancer therapeutics

Sanjay Kumar Paul¹, Abdelmadjid Guendouzi^{2,3}, Abdelkrim Guendouzi⁴, Rajen Haldar^{5*}

ABSTRACT

Cancer cells require high NAD⁺ levels to sustain their rapid growth, relying primarily on the salvage pathway for NAD⁺ replenishment. The overexpression of nicotinamide phosphoribosyltransferase (NAMPT), a key enzyme in this pathway, correlates with the increased NAD⁺ demand in cancer cells, making it a critical target for anticancer drug development. Moreover, a few small-molecule inhibitors targeting NAMPT have shown promise in restricting tumor growth, further establishing NAMPT as a potential therapeutic target in cancer treatment. This computational study aims to identify potential NAMPT inhibitors that can effectively suppress the over-activated NAD⁺ salvage pathway in cancer cells, thereby inhibiting tumor growth. Instead of developing novel inhibitors from scratches, this study specifically aims to screen approved drugs using computational methods to find a repurposable drug that binds strongly to NAMPT, offering a faster and cost-effective approach to cancer treatment. Initially, molecular docking was employed to screen 1,615 approved drugs, followed by a detailed examination of drug-protein interactions using advanced computational techniques, including molecular dynamics simulation, principal component analysis, and MM-PBSA. Among the screened compounds, posaconazole, an antifungal drug, emerged as a top candidate with a high affinity for the NAMPT active site, surpassing a known synthetic NAMPT inhibitor. Molecular dynamics simulations and MMPBSA confirmed the stability of the NAMPT-posaconazole complex, further supporting its potential as a NAMPT inhibitor. However, further in vitro, in vivo, and clinical validation is essential to confirm its anticancer efficacy.

Keywords: NAMPT, Cancer therapy, Computational drug repurposing, Posaconazole, Molecular docking.

Indian Journal of Physiology and Allied Sciences (2025);

DOI: 10.55184/ijpas.v77i02.469

ISSN: 0367-8350 (Print)

INTRODUCTION

Anticancer drug development strategies are primarily based on finding ways to specifically kill cancer cells while avoiding damage to the normal cells.^{1,2} For example, cancer cells require specific nutrients, such as glucose, amino acids, fatty acids, nucleotides, vitamins, minerals, and cofactors, in higher amounts than normal cells to support their rapid growth and proliferation. Therefore, cancer cells use metabolic reprogramming strategies to fulfill their increased energy demands and biosynthetic needs.^{3,4} These altered metabolisms are viewed as signatures of cancer cells and have been explored to inhibit cancer growth and proliferation in various studies selectively.⁵

Nicotinamide adenine dinucleotide (NAD⁺) is a coenzyme consisting of nicotinamide mononucleotide (NMN) linked to adenosine monophosphate (AMP). It plays a crucial role in various cellular processes like energy metabolism, redox reactions, DNA repair, genomic stability, regulation of sirtuins, and cell signaling.^{6,7} Because of its important roles in cellular metabolism, cancer cells require more NAD⁺ than normal cells, and in concert, they synthesize more NAD⁺ by upregulating the NAD⁺ synthetic pathways.⁸

NAD⁺ is synthesized mainly by the de novo and salvage pathways in mammals. The de novo pathway utilizes simple nutrients, such as L-tryptophan or nicotinic acid (NA), as precursors and converts them into NAD⁺ through a series of enzymatic reactions. In the salvage pathway, the by-product of NAD⁺ metabolism, such as nicotinamide

¹Department of Zoology, Rammohan College, 102/1- Raja Rammohan Sarani, Kolkata- 700009, West Bengal, India.

²Center for Research in Pharmaceutical Sciences (CRSP), Ali Mendjeli, 25000 Constantine, Algeria.

³Ecole Normale Supérieure ENS Constantine, Constantine.

⁴Department of Chemistry, Faculty of Sciences. University of Saida, Dr Moulay Tahar, Algeria.

⁵Department of Physiology, University of Calcutta, 92, A.P.C. Road, Kolkata- 700 009, India.

***Corresponding author:** Rajen Haldar, Department of Physiology, University of Calcutta, 92, A.P.C. Road, Kolkata- 700 009, India, Email: rhphys@caluniv.ac.in

How to cite this article: Paul SK, Guendouzi A, Guendouzi A, Haldar R. Computational drug repurposing: Posaconazole emerges as a potent NAMPT inhibitor, offering promise for precision cancer therapeutics. *Indian J Physiol Allied Sci* 2025;77(2):61-69.

Conflict of interest: None

Submitted: 10/11/2024 **Accepted:** 18/05/2025 **Published:** 20/06/2025

(NAM), is recycled to form NAD⁺, and thus, the balance between NAD⁺ consumption and breakdown is maintained.⁹ Moreover, it is assumed that the salvage pathway is the major source of NAD⁺ within the cells.¹⁰ The rate-limiting step in the NAD⁺ salvage pathway is the conversion of nicotinamide (NAM) to nicotinamide mononucleotide (NMN), which is subsequently converted to NAD⁺. This step regulates the availability of NMN, thereby serving as a key bottleneck in the salvage pathway. The enzyme that catalyzes

this rate-limiting in the salvage pathway is nicotinamide phosphoribosyltransferase (NAMPT). It converts nicotinamide (NAM) to nicotinamide mononucleotide (NMN) using 5-phosphoribosyl-1-pyrophosphate as a substrate (Figure 1A). This is probably why various cancer cells with increased NAD^+ metabolism show elevated expression of NAMPT.¹¹ Furthermore, the dependency of the cancer cells on NAMPT for NAD^+ synthesis has made NAMPT an attractive target for anticancer drug design.¹²

The crystal structure of mammalian NAMPT (Figure 1B) revealed that it is a dimeric enzyme containing two tunnel-like active sites at the dimer interface. After binding of nicotinamide (NAM) and phosphoribosyl pyrophosphate (PRPP) substrates at the active site, NAMPT hydrolyzes one ATP molecule and becomes autophosphorylated at His247. The additional negative charge arising from histidine phosphorylation is possibly used to cleave PRPP into positively charged oxacarbenium intermediate and pyrophosphate. The oxacarbenium intermediate then reacts with nicotinamide to form NMN.¹³ The crystal structures also revealed that the nicotinamide is sandwiched between the stacked aromatic rings of Phe 193 and Tyr 18 from two different monomers and occupies the same site even after formation of NMN through conjugation with phosphoribosyl group.¹⁴ Hence, this Pi-Pi stacking is considered the most important part of substrate binding. A hydrogen bond between Asp219 and the amide group of nicotinamide is important for substrate specificity, *i.e.*, distinguishing between nicotinamide and nicotinic acid; nevertheless, a mutational study revealed that this interaction has negligible impact on reaction catalysis.¹⁵

Several NAMPT inhibitors have been developed as potential anticancer agents.¹⁶ In 2002, the pyridine derivative FK866 was the first reported NAMPT inhibitor, exhibiting strong

preclinical efficacy but encountering toxicity issues.¹⁷ The cyanoguanidine derivative CHS828 advanced to clinical trials¹⁸ and was later modified into GMX1777, which improved solubility.¹⁹ Another inhibitor, GEN617, containing an amide group, demonstrated potent activity but was associated with retinal toxicity,²⁰ leading to the development of LSN3154567, which exhibited reduced toxicity.²¹ Additionally, A1293201, featuring an isoindoline head group, showed strong preclinical efficacy.²² Most recently, OT-82, developed by OncoTaris, entered Phase I clinical trials in 2019, underscoring ongoing efforts to refine NAMPT-targeted therapies.²³ Moreover, targeting NAMPT in combination with chemotherapeutic agents can enhance the effectiveness of these treatments.²⁴ However, despite considerable efforts, none of the inhibitors developed so far have gained clinical approval for their application in cancer therapy targeting NAMPT. Hence, it is imperative to explore the avenue of drug repurposing in this context.^{25,26} This study aims to identify approved drugs that may potentially inhibit NAMPT. The investigation utilizes computational techniques, including molecular docking, molecular dynamics simulation, and MM-PBSA binding energy calculation, to screen approved drugs and analyze drug-protein interactions.

MATERIALS AND METHODS

Molecular Docking

A crystallographic structure of human NAMPT (PDB ID: 4KFN) complexed with a synthetic inhibitor (1QR) was downloaded from the Protein Data Bank (<https://www.rcsb.org/>).²⁷ The PDB ID was selected based on the resolution of the structure (1.60 Å) and the IC_{50} value of the bound inhibitor (IC_{50} -9 nM). The 3D structures of 1615 FDA-approved drugs were downloaded from the ZINC database (<https://zinc.docking.org/>)²⁸ in SDF format and converted into MOL2 format through open babel.²⁹ Molegro Virtual Docker (Version 7.0.0) was harnessed based on the differential evolution algorithm and a cavity prediction algorithm³⁰ to screen the FDA-approved drugs.³¹ In the beginning, 1QR was redocked to the active site of NAMPT to verify the suitability of the docking software and to standardize the docking protocol. The PDB structure of NAMPT was first imported into the MVD workspace and then processed for docking by repairing the altered residues and removing all hetatm, including water molecules. The cavity prediction algorithm was used to locate the active site, and a search space of 20 Å radius (center X: 11.29 center Y: 7.86 center Z: 3.62) was defined, enclosing one of the two active site cavities (volume: 476.16 Å³). Subsequently, the drugs were imported into the workspace and prepared or minimized by default settings. The docking parameters used were - run number: 10, maximum iterations: 1500, maximum poses returned: 5, and RMSD threshold for clustered poses: 1 Å. The docking scores in a text file and each drug's top five docked poses are automatically saved in an output file. In molecular docking studies, employing multiple scoring functions to evaluate docked poses—known as consensus

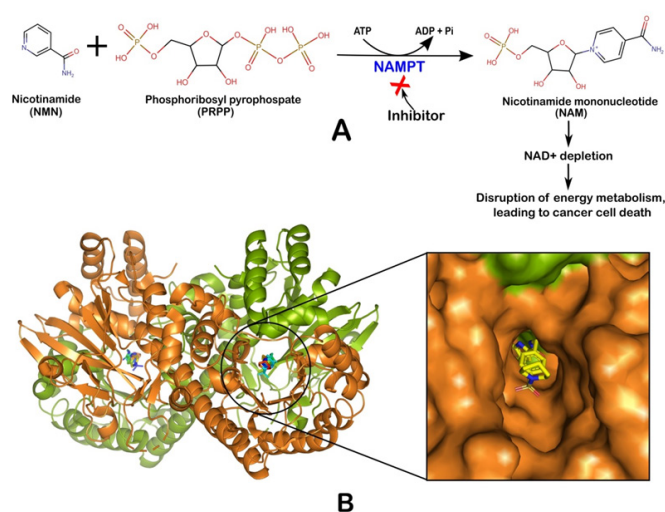


Figure 1: (A) Schematic representation of NAMPT-mediated catalytic conversion of NAM to NMN and mechanism of anticancer activity of NAMPT inhibitor. (B) 3D structure of human NAMPT homodimer and its tunnel-like active site

scoring—can enhance the accuracy of predicting the most favorable binding conformations. This approach mitigates the limitations of relying on a single scoring function and improves the reliability of docking results.³² MVD uses three different scoring functions (Moldock score, Rerank score, and Plant score) to rank the docked poses, and in this study, the pose that scored highest, at least in two scoring functions, was considered the top pose.

Molecular Dynamics Simulation

The best-docked poses obtained from molecular docking studies in a complex with NAMPT were used as input for molecular dynamics simulation. GROMACS 2023 simulation package³³ was used for MD simulations over 250 ns using CHARMM36 force field.³⁴ The topology of ligands was generated employing the SwissParam web server (<http://swissparam.ch/>).³⁵ Then, the protein complex was enclosed in a cubic simulation box with a minimum distance of 1 nm to the box edge, and then the system was solvated with TIP3P water molecules.³⁶ Overall, the system was neutralized by adding sodium/chlorine ions and minimized using the Steepest Descent algorithm for 5000 steps. The convergence was achieved within the maximum force, $F_{\max} < 1000$ (KJ mol⁻¹ nm⁻¹). To ensure full convergence of the system for the production run, the system was equilibrated for 2ns under the NVT ensemble (time steps=0.2 fs) and followed by the NPT ensemble (time step = 0.1 fs) at 300 K temperature. The system's temperature and pressure were maintained using the V-rescale thermostat³⁷ and applying the Parrinello–Rahman barostat at 1.0 bar. Periodic boundary conditions were applied in all x, y, and z directions. The equilibrated systems were subjected to an unrestrained production run, maintaining constant temperature and pressure for 250 ns. The LINCS algorithm kept all bond lengths rigid at ideal bond lengths. Non-bonded interactions were calculated using the verlet scheme. Interactions within a short-range cutoff of 1.2nm were calculated in each time step. The electrostatic interactions and forces to account for a homogeneous medium outside the long-range cutoff used Particle Mesh Ewald (PME).³⁸

The MD simulation's results were analyzed by calculating the root mean square deviation (RMSD), root mean square fluctuation (RMSF), radius of gyration (ROG), and solvent accessible surface area (SASA). Principal component analysis (PCA) and free energy landscape (FEL) analyses were performed on the last 100 ns simulation trajectory.

Principal Component Analysis and Free Energy Landscape

Principal component analysis (PCA) is a statistical technique employed to evaluate the collective motion within biological macromolecules during molecular dynamic simulations. PCA's essence is reducing dataset dimensions while retaining pivotal information encapsulated within eigenvectors.^{39,40} This process was harnessed to assess the flexibility of the

protein in the presence of 1QR and posaconazole. The covar module of gromacs was used to calculate the covariance matrix for each complex. Then, the ana eig module was used to generate a 2D projection of the first two principal components (PC1 and PC2). The 2D projection defines the conformational space of the complexes along the trajectory. Gibbs free energy landscapes were plotted using the data present in 2d projection.xvg files. The landscape depicts the free energy state of the conformations of the protein complex within the conformational space and thus can be used to access the journey of the complex toward its stability.⁴¹

MMPBSA Binding Energy Calculation

This study employed gmx_MMPBSA - a tool introduced by Valdés-Tresanco *et al.*⁴² for conducting end-state binding free energy calculations based on GROMACS molecular dynamics trajectories using a single trajectory protocol. Notably, gmx_MMPBSA seamlessly integrates the MMPBSA.py python script⁴³ from the amber package along with relevant programs from GROMACS. This amalgamation allows for the comprehensive calculation of binding free energies for non-covalently bound complexes. To extract meaningful insights, we selectively utilized 100 frames from the last 10 ns of the MD trajectory for each complex, employing a 100-picosecond interval between the frames. This meticulous frame selection strategy ensures a representative sampling of the complex's dynamic behavior during the critical phase of interaction. The binding free energy for a complex is estimated as follows:

$\Delta G_{bind} = G_{com} - (G_{rec} + G_{lig})$, where G is the free energy
In gmx_MMPBSA, the enthalpic contribution (ΔH) of the free energy is usually calculated. Enthalpy can be decomposed into different energy terms;

$\Delta H = \Delta E_{MM} + \Delta G_{SOL}$
Where, $\Delta E_{MM} = \Delta E_{bonded} + \Delta E_{nonbonded}$
 $= (\Delta E_{bond} + \Delta E_{angle} + \Delta E_{dihedral}) + (\Delta E_{ele} + \Delta E_{vdW})$
 ΔE_{bonded} , also known as internal energy, and $\Delta E_{nonbonded}$ include the van der Waals and electrostatic contributions.

And $\Delta G_{SOL} = \Delta G_{polar} + \Delta G_{non-polar}$
 $= \Delta G_{PB/GB} + \Delta G_{non-polar}$

The polar contribution is estimated through the PB/GB model, and the non-polar contribution is most frequently referred to as the SASA (solvent-accessible surface area) contribution.

RESULT AND DISCUSSION

We conducted a computational study to find out a few approved drugs with anticancer properties. For that, we screened 1615 approved drugs by testing their interaction with human NAMPT. The drugs that performed better than a known inhibitor (IC50- 9 nM) in the molecular docking experiment were considered potential inhibitors. These drugs were further analyzed for their binding stability through molecular dynamics simulations and MMBSA binding energy calculation. A schematic representation of the study design is shown in Figure 2.

Molecular Docking

A total of 1615 approved drugs archived in the ZINC database were virtually screened for their NAMPT binding potential through molecular docking. Molecular docking predicts the possible molecular interaction of ligands with the active site residues of protein and ranks the ligands based on their binding potential. In this study, we primarily docked the known synthetic inhibitor (1QR), which was co-complexed with the NAMPT in PDB ID: 4JNK, to test the suitability of docking software and docking protocol. The calculated RMSD between the best pose obtained from the docking study and the crystallographic pose is 1.8 Å, which indicates that the poses are very similar. The docking method has perfectly predicted the crystallographic pose.

Then, using the same docking protocol, approved drugs were docked in the active site of NAMPT. The obtained score of the best pose of 1QR has been set as a threshold value for comparison and screening. Since MVD ranks the same docked, pose thrice using three different scoring functions ((Moldock score, Rerank score, and Plant score), the approved drugs that crossed all three threshold scores were only considered potential binders of NAMPT. However, the selection of such stringent screening conditions resulted in identifying only four approved drugs that could bind NAMPT more strongly than the 1QR. The scores of the 1QR and four shortlisted approved drugs (Lapatinib, Nilotinib, Posaconazole, and Abemaciclib) are listed in Table 1 for comparison. Moreover, the two-dimensional structures of 1QR and four approved drugs are presented in Figure 3. A visual inspection of the 2D structures of the four approved drugs revealed that they are elongated molecules, similar

Table 1: The scores of the known inhibitor (1QR) and the top four approved drugs were obtained from molecular docking using molegrovirtual docker (MVD)

S No.	Ligand	Group	Plant score	Moldock score	Rerank score
1	1QR	Synthetic inhibitor	-100.85	-149.30	-121.15
2	Lapatinib	Anticancer drug	-107.83	-160.36	-133.15
3	Nilotinib	Anticancer drug	-107.61	-160.48	-128.56
4	Posaconazole	Antifungal drug	-122.56	-160.36	-133.02
5	Abemaciclib	Anticancer drug	-101.21	-153.11	-123.66

to 1QR, an important feature that makes them primarily accessible to the tunnel-like active site of NAMPT. Out of the four high-scoring approved drugs, three drugs (lapatinib, nilotinib, and abemaciclib) belong to anticancer drug groups, and one drug (posaconazole) belongs to the antifungal drug group. Since the main objective of this study is to identify a repurposable approved drug for safe cancer therapy, we further explored the interaction of posaconazole with NAMPT and evaluated its inhibitory potential on NAMPT using other in-silico methods.

Achieving high scores in docking studies depends on the binding mode of the ligand and the nature of interaction with the active site residues.⁴⁴ Moreover, a few key interactions are necessary for ligand-induced inhibition of the target protein.⁴⁵ Therefore, it's important to explore the protein-ligand interaction to assess the possible consequence of ligand binding in the protein active site and this interaction itself as a criterion for screening the potential inhibitor.

In Figure 4, the 2D and 3D interaction of two known inhibitors (1QR & FK866) and posaconazole with NAMPT are presented for comparative inspection of interactive residues, type of interaction, and binding pattern of the drugs. The protein-ligand interaction diagrams show that the bicyclic azaindole portion of 1QR and pyridine portion of FK866 occupied the NAM binding site of NAMPT and were stacked between the Tyr18' and Phe193 side chains of the protein. The Benzyl group in 1QR interacted with His191, Ser241, Val 242, and Ile 351 of a hydrophobic groove within the tunnel-like active site pocket.⁴⁶ A few other residues of this hydrophobic groove play an important role in binding other scaffold-based inhibitors. For example, FK866 was reported to interact with Ala 244, Ile 309, and Ala 379 within this hydrophobic region, in addition to stacking its pyridine moiety between Tyr18' and Phe193. Moreover, these interactions are considered key to FK866's specificity toward NAMPT.⁴⁷ As per the docking study, the phenyl group of posaconazole may occupy the NAM binding site stacked between the Tyr18' and Phe193 and thus might competitively inhibit the binding of NAM in the active site. The methoxy phenyl moiety of posaconazole interacts

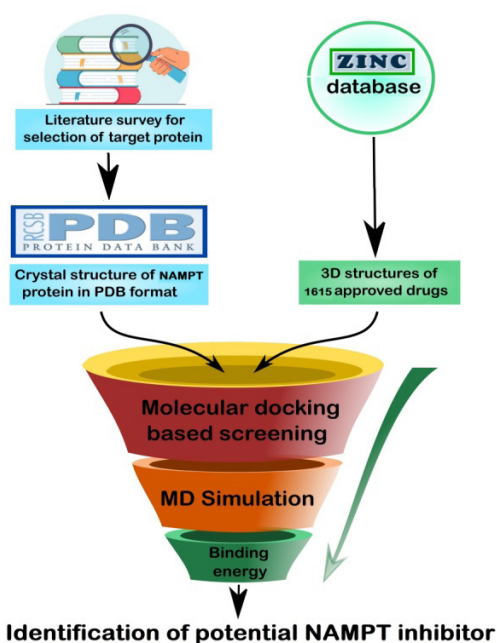


Figure 2: Schematic representation of the study workflow, illustrating top inhibitor selection via molecular docking and validation through molecular dynamics and MM-GBSA analysis

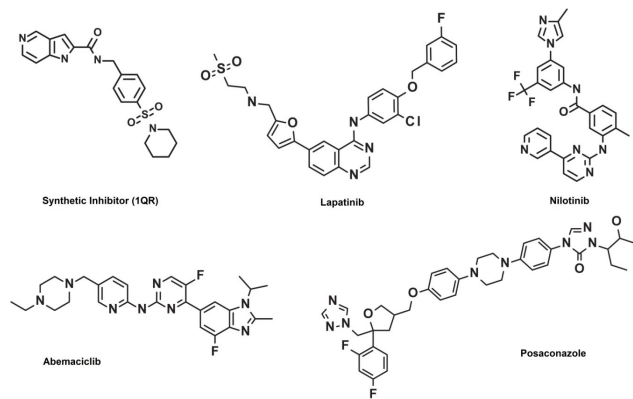


Figure 3: 2D structures of the known synthetic inhibitor (1QR) of NAMPT and four top-scored approved drugs as per molecular docking-based screening

with Ile 309, Ile 351, and Ala 379 of the hydrophobic groove, as seen in case FK866. A few additional residues like Arg 196, Gln 305, and Pro 307 also interact with posaconazole. However, it is evident from the comparison that the binding pose and interaction pattern of posaconazole within the active site of NAMPT are very similar to the two known inhibitors. This suggests that posaconazole may be a potential inhibitor of NAMPT. However, a docking experiment cannot predict whether the docked pose will maintain these interactions or form a stable complex with NAMPT. Therefore, NAMPT, in combination with the known inhibitor and posaconazole, was subjected to molecular dynamics simulation for a comparative study.

Molecular Dynamics Simulation

To evaluate and compare the dynamic behavior and stability of the NAMPT-posaconazole complex with that of the NAMPT-

1QR complex under normal physiological conditions, we conducted molecular dynamics (MD) simulations on these two complexes. The simulations were carried out for 250 nanoseconds. Upon completing the MD simulation, we extracted key parameters from the trajectory file, including RMSD, RMSF, SASA, and ROG.

The interaction between a ligand and a protein's active site induces gradual conformational changes in both the ligand and the protein.⁴⁸ To assess these changes, we utilized RMSD, which estimates conformational variations by comparing subsequent conformations to the initial reference conformation. Specifically, we calculated the RMSD separately for the backbone of NAMPT and its associated ligand for each complex. The GROMACS program was employed for this purpose, providing insights into the patterns of conformational changes in both the protein and the ligand during the binding process (Figure 5). The RMSD plots generated for the NAMPT backbone indicate that the protein reached a stable state at ~25 ns in both NAMPT-1QR and NAMPT-posaconazole complexes. RMSD fluctuations were confined within a very narrow range in the rest of the simulation period. The average RMSD fluctuation values for the NAMPT backbone in the complex with 1QR and posaconazole are calculated as 0.25 and 0.24, respectively. The RMSD trajectory of 1QR and posaconazole demonstrate their confinement within the active site pocket of NAMPT throughout the 250 nanoseconds simulation. Both of them achieved dynamic equilibrium at the beginning of the simulation, indicating that the obtained docked poses correctly predicted the optimum conformation of 1QR and posaconazole within the binding pocket of NAMPT. Moreover, such stable ligand RMSD trajectories underscore the persistent interaction of the compounds within the critical binding site of NAMPT, affirming their sustained presence and

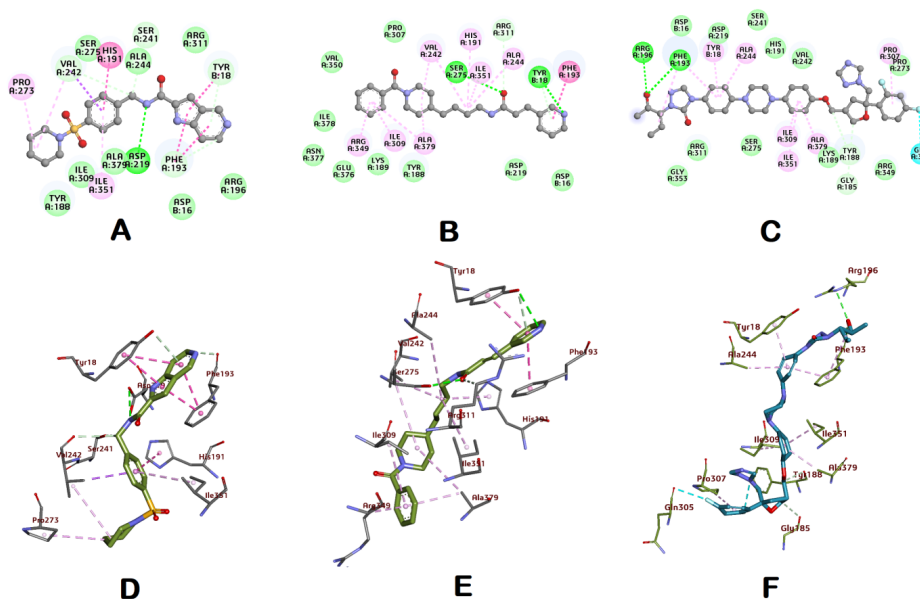


Figure 4: 2D and 3D representations of interactions between NAMPT active site residues with two known inhibitors (1QR-A & D, FK866- B & E) and posaconazole (C & F), respectively

adherence to the desired conformational parameters. The nuanced dynamics, particularly the stabilization patterns observed in these ligands, contribute valuable insights into their binding kinetics and reinforce their potential as effective inhibitors within the studied timeframe.

The analysis of RMSF for alpha-carbon atoms of the dimeric NAMPT, as depicted in Figure 6A, revealed a consistent fluctuation pattern in both NAMPT-1QR and NAMPT-posaconazole complexes. In each complex, elevated fluctuations were particularly evident in two terminal loop regions (1-21 and 481-489) and two intermediate loop regions (40-60 and 414-430) of subunit A. The first terminal loop (1-21) from a part of the 2nd active site where the ligand was not docked. The remaining regions are outside the active site and do not directly participate in ligand binding. Additionally, mild fluctuations were noted in two loop regions (233-246 and 275-282), forming a part of the side wall of the 1st active site with the docked ligand. A loop region (490-511 or 1' - 21') from the B subunit, which participates in forming the 1st active sites, also shows mild fluctuations to accommodate the ligands. However, it's noteworthy that other regions surrounding the active site exhibited limited fluctuation. This observation implies that the active site residues within the binding pocket maintain stable interactions with the 1QR and posaconazole. The analysis indicated that the fluctuations observed in these critical regions did not compromise the stability of the protein-ligand complexes. Importantly, the RMSF profiles hinted at similar conformational fluctuations when compared between the backbone of the NAMPT-posaconazole and the NAMPT-1QR complexes. This similarity in conformational dynamics underscores the consistency in the behavior of posaconazole compared to the established inhibitor.

The 250 ns simulation trajectories of NAMPT-1QR and NAMPT-posaconazole complexes underwent further analysis using radius gyrations (ROG) to track changes in their compactness (Figure 6B). The calculated average Rog values for NAMPT-1QR and NAMPT-posaconazole complexes are 2.959Å and 2.961Å, respectively. Remarkably, in each case, Rog exhibited minimal fluctuations within 1Å, signifying the sustained compactness of both complexes throughout the simulation.

The post-simulation analysis also included SASA calculations, offering insights into protein thermodynamic stability. SASA analysis, conducted meticulously over the 250ns trajectory (Figure 6D), aimed to anticipate conformational changes influenced by water interactions. Average SASA values for NAMPT-1QR and NAMPT-posaconazole were 367.419 and 384.141 nm², respectively. Notably, the NAMPT-posaconazole complex demonstrated SASA values close to the NAMPT-1QR complex, indicating comparable solvent exposure. This suggests that, despite potential dynamic changes, both complexes maintained a consistent level of thermodynamic stability throughout the simulation.

Hydrogen bond analysis was performed to evaluate the interactions between the active site residues of the NAMPT

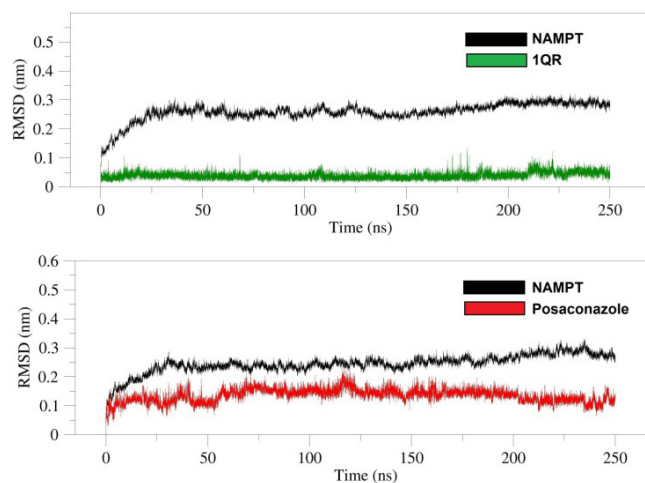


Figure 5: RMSD trajectories of the backbone of the NAMPT, known inhibitor (1QR), and posaconazole over a duration of 250 ns

and two drugs- the control (1QR) and the test (posaconazole), over a 250 ns simulation. Both drugs exhibited a maximum of five hydrogen bonds; however, the high frequency of H-bond formation suggests that hydrogen bonding is a key stabilizing factor in their binding along with other interactions, such as hydrophobic or van der Waals forces.

Principal Component Analysis and Free Energy Landscape

PCA proves invaluable in extracting insights into the conformational sampling of protein structures.⁴⁹ The outcomes of the PC analysis yielded valuable insights into the dynamic flexibility of the protein during interactions with its corresponding ligands. Figure 6B vividly illustrates the first two eigenvectors projected onto NAMPT-1QR and NAMPT-posaconazole complexes. The 2D projection unequivocally reveals a shared conformational space among these complexes, harmonizing seamlessly with the native protein's inherent conformational arrangement. This observation underscores a commonality in the structural dynamics of these complexes, suggesting a conserved interaction pattern. When expressed in terms of free energy states, the sampled conformations collectively form a free energy landscape (FEL), unveiling the trajectory of protein complexes toward their global minima.⁵⁰ The FEL contains one or more funnel-shaped energy basins with a slope that guides the protein complex toward the global minima.⁵¹ At the bottom of the funnel-shaped energy basin, more than one metastable conformational state usually remains present.⁵² We examined the stability of NAMPT-ligand complexes during MD simulations by constructing a Free Energy Landscape (FEL) utilizing the initial two principal components (PCs). The color gradient employed in the depiction signifies the free energy states of the conformations (Figures 7A and 7B). Notably, the most stable conformational state is represented by blue color. The FEL plots of the NAMPT- 1QR and NAMPT-posaconazole complexes show four and three global minima, respectively.

Table 2: Calculated binding free energies of 1QR and posaconazole (kJ/mol).

Complex name	ΔG	vdW energy	Electrostatic energy	Polar solv Energy	Non-polar solv energy
1QR	-18.42 ± 6.55	-47.48 ± 3.05	-56.61 ± 4.64	90.33 ± 8.13	-4.65 ± 0.08
Posaconazole	-19.18 ± 6.45	-75.67 ± 3.56	-108.62 ± 11.21	172.30 ± 10.38	-7.19 ± 0.17

Values are mean \pm standard deviation.

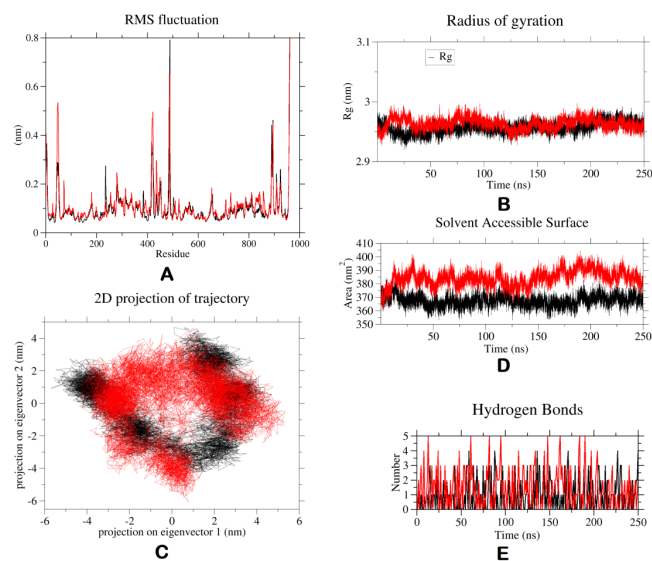


Figure 6: Root Mean Square Fluctuation (RMSF) of the complexes (A), Radius of gyration of the complexes (B), SASA plot of the complexes (D), H bond analysis between active site residues and ligands of the complexes (E) during 250 ns simulation. 2D projection of the motion of two NAMPT-ligand complexes constructed by plotting the first two principal components (PC1 and PC2) in the conformational space (C). NAMPT-1QR complex (Black) and NAMPT-posaconazole complex (Red)

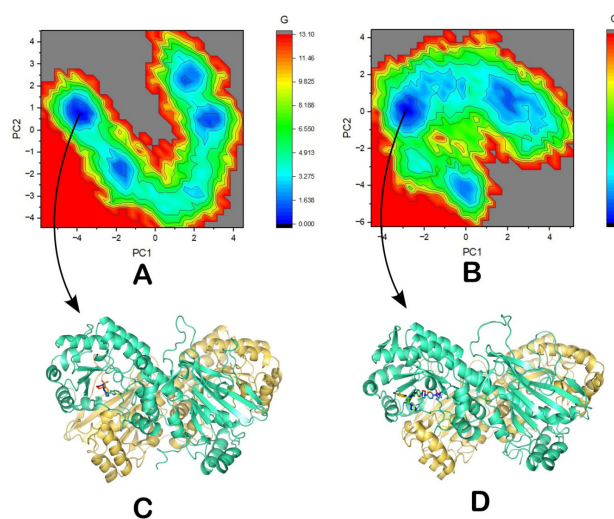


Figure 7: The free energy landscapes (FEL) of NAMPT- 1QR (A) and NAMPT- posaconazole complexes (B). Visual comparison of the minima structures of NAMPT complexed with 1QR (C) and posaconazole (D)

The presence of well-defined energy basins indicates that the complexes could attain stable states during the MD simulation. We also extracted one representative stable conformation of NAMPT- 1QR and NAMPT-posaconazole complexes from the global minima region for visualization (Figures 7C and 7D). The diagram shows that the ligands remained within the active site pocket of stable NAMPT and maintained interactions with active site residues.

Binding Free Energy Using MM-PBSA Approach

The ΔG binding free energy of 1QR and posaconazole was calculated from the last 10 ns of the MD simulation trajectories using the MM-PBSA approach. Calculated average ΔG bind values and standard deviations are given in Table 2. The table shows that the ΔG bind value of the NAMPT-1QR complex is -18.42 kJ/mol, and the ΔG bind value of the NAMPT-posaconazole complex is -19.18 kJ/mol, i.e., the binding affinity of posaconazole for NAMPT is slightly more than the binding affinity of the 1QR. Moreover, the table shows that the polar solvation energy of the NAMPT- posaconazole complex is much higher than the NAMPT- 1QR complex. However, like the NAMPT-1QR complex, the high negative van der Waals and electrostatic contribution compensated for the polar solvation energy.

CONCLUSION

In this computational investigation, employing molecular docking analysis, we have identified one approved drug, posaconazole, which exhibits promising potential to bind to the active site pocket of NAMPT with high affinity. In molecular dynamics simulations, posaconazole consistently maintained stable binding within the active site pocket of NAMPT, reminiscent of the known inhibitor. Moreover, the binding energy of posaconazole surpassed the binding energies of 1QR, which boasts an IC_{50} value of 9 nM. Therefore, the posaconazole warrants further exploration through *in-vitro* and *in-vivo* experiments to validate its potential efficacy. Notably, as a member of a widely prescribed antifungal drug class, posaconazole could be repurposed for cancer therapy across a broader population, minimizing the likelihood of additional side effects.

AUTHORS' CONTRIBUTIONS

Sanjay Kumar Paul designed the study and methods. Sanjay Kumar Paul, Abdelmadjid Guendouzi and Abdelkrim Guendouzi carried out the experiment. Sanjay Kumar Paul and Rajen Haldar analyzed the results of the experiment. Sanjay Kumar Paul and Rajen Haldar drafted the manuscript.

All authors have approved the final manuscript.

FUNDING

The author(s) reported there is no funding associated with the work featured in this article

REFERENCES

- Pucci C, Martinelli C, Ciofani G. Innovative approaches for cancer treatment: current perspectives and new challenges. *Ecancelmedscience*. 2019;13:961. DOI: 10.3332/ecancer.2019.961.
- DeNicola GM, Cantley LC. Cancer's fuel choice: new flavors for a picky eater. *Mol Cell*. 2015;60(4):514-23. DOI: 10.1016/j.molcel.2015.10.018.
- De Berardinis RJ, Chandel NS. Fundamentals of cancer metabolism. *Sci Adv*. 2016;2(5):e1600200. DOI: 10.1126/sciadv.1600200.
- Schiliro C, Firestein BL. Mechanisms of Metabolic Reprogramming in Cancer Cells Supporting Enhanced Growth and Proliferation. *Cells*. 2021;10(5):1056. DOI: 10.3390/cells10051056.
- Stine ZE, Schug ZT, Salvino JM, Dang CV. Targeting cancer metabolism in the era of precision oncology. *Nat Rev Drug Discov*. 2021;21(2):141-62. DOI: 10.1038/s41573-021-00339-6.
- Amjad S, Nisar S, Bhat AA, et al. Role of NAD⁺ in regulating cellular and metabolic signaling pathways. *Mol Metab*. 2021;49:101195. DOI: 10.1016/j.molmet.2021.101195.
- Yaku K, Okabe K, Hikosaka K, Nakagawa T. NAD Metabolism in Cancer Therapeutics. *Front Oncol*. 2018;8:622. DOI: 10.3389/fonc.2018.00622.
- Navas LE, Carnero A. NAD⁺ metabolism, stemness, the immune response, and cancer. *Signal Transduct Target Ther*. 2021;6(1):20. DOI: 10.1038/s41392-020-00354-w.
- Rongvaux A, Andris F, Van Gool F, Leo O. Reconstructing eukaryotic NAD metabolism. *Bioessays*. 2003;25(7):683-90. DOI: 10.1002/bies.10297.
- Houtkooper RH, Cantó C, Wanders RJ, Auwerx J. The Secret Life of NAD⁺: An old metabolite controlling new metabolic signaling pathways. *Endocr Rev*. 2010;31(2):194-223. DOI: 10.1210/er.2009-0026.
- Kennedy BE, Sharif T, Martell E, Dai C, Kim Y, Lee PWK, Gujar SA. NAD⁺ salvage pathway in cancer metabolism and therapy. *Pharmacol Res*. 2016;114:274-83. DOI: 10.1016/j.phrs.2016.10.027.
- Sampath D, Zabka TS, Misner DL, O'Brien T, Dragovich PS. Inhibition of nicotinamide phosphoribosyltransferase (NAMPT) as a therapeutic strategy in cancer. *Pharmacol Ther*. 2015;151:16-31. DOI: 10.1016/j.pharmthera.2015.02.004.
- Wang T, Zhang X, Bheda P, Revollo JR, Imai SI, Wolberger C. Structure of Nampt/PBEF/visfatin, a mammalian NAD⁺ biosynthetic enzyme. *Nat Struct Mol Biol*. 2006;13(7):661-2. DOI: 10.1038/nsmb1114.
- Takahashi R, Nakamura S, Nakazawa T, et al. Structure and reaction mechanism of human nicotinamide phosphoribosyltransferase. *J Biochem*. 2010;147(1):95-107. DOI: 10.1093/jb/mvp152.
- Galli U, Colombo G, Travelli C, Tron GC, Genazzani AA, Grolla AA. Recent advances in NAMPT inhibitors: A novel immunotherapeutic strategy. *Front Pharmacol*. 2020;11:531540. DOI: 10.3389/fphar.2020.00656.
- Wei Y, Xiang H, Zhang W. Review of various NAMPT inhibitors for the treatment of cancer. *Front Pharmacol*. 2022;13:970553. DOI: 10.3389/fphar.2022.970553.
- Hasmann M, Schemainda I. FK866, a highly specific noncompetitive inhibitor of nicotinamide phosphoribosyltransferase, represents a novel mechanism for induction of tumor cell apoptosis. *Cancer Res*. 2003;63(4):743-9.
- Olesen UH, Christensen MK, Björkling F, et al. Anticancer agent CHS-828 inhibits cellular synthesis of NAD. *Biochem Biophys Res Commun*. 2008;367(4):799-804. DOI:10.1016/j.bbrc.2008.01.019.
- Beuparlant P, Bédard D, Bernier C, et al. Preclinical development of the nicotinamide phosphoribosyl transferase inhibitor prodrug GMX1777. *Anticancer Drugs*. 2009;20(5):346-54. DOI:10.1097/cad.0b013e3283287c20.
- Zheng X, Bauer P, Baumeister T, et al. Structure-based discovery of novel amide-containing nicotinamide phosphoribosyltransferase (NAMPT) inhibitors. *J Med Chem*. 2013;56(16):6413-33. DOI:10.1021/jm4008664.
- Zhao G, Green CF, Hui YH, et al. Discovery of a highly selective NAMPT inhibitor that demonstrates robust efficacy and improved retinal toxicity with nicotinic acid coadministration. *Mol Cancer Ther*. 2017;16(12):2677-88. DOI:10.1158/1535-7163.mct-16-0674.
- Wilsbacher JL, Cheng M, Cheng D, et al. Discovery and characterization of novel nonsubstrate and substrate NAMPT inhibitors. *Mol Cancer Ther*. 2017;16(7):1236-45. DOI:10.1158/1535-7163.mct-16-0819.
- Korotchkina L, Kazyulkin D, Komarov PG, et al. OT-82, a novel anticancer drug candidate that targets the strong dependence of hematological malignancies on NAD biosynthesis. *Leukemia*. 2020;34(7):1828-39. DOI:10.1038/s41375-019-0692-5.
- Roulston A, Shore GC. New strategies to maximize therapeutic opportunities for NAMPT inhibitors in oncology. *Mol Cell Oncol*. 2016;3(1):e1052180. DOI: 10.1080/23723556.2015.1052180.
- Paul SK, Dutta Chowdhury K, Dey SR, Paul A, Haldar R. Exploring the possibility of drug repurposing for cancer therapy targeting human lactate dehydrogenase A: a computational approach. *J Biomol Struct Dyn*. 2022;40(9):3411-22. DOI: 10.1080/07391102.2022.2158134.
- Pushpakom S, Iorio F, Eyers PA, et al. Drug repurposing: progress, challenges and recommendations. *Nat Rev Drug Discov*. 2018;18(1):41-58. DOI: 10.1038/nrd.2018.168.
- Berman HM, Westbrook J, Feng Z, et al. The protein data bank. *Nucleic Acids Res*. 2000;28(1):235-42. DOI: 10.1093/nar/28.1.235.
- Irwin JJ, Shoichet BK. ZINC – A free database of commercially available compounds for virtual screening. *J Chem Inf Model*. 2005;45(1):177-82. DOI: 10.1021/ci049714.
- O'Boyle NM, Banck M, James CA, Morley C, Vandermeersch T, Hutchison GR. Open Babel: An open chemical toolbox. *J Cheminform*. 2011;3(10):33. DOI: 10.1186/1758-2946-3-33.
- Thomsen R, Christensen MH. MolDock: A new technique for high-accuracy molecular docking. *J Med Chem*. 2006;49(11):3315-21. DOI: 10.1021/jm051197e
- Bitencourt-Ferreira G, de Azevedo WF. Molegro virtual docker for docking. *Methods Mol Biol*. 2019;2053:149-67. DOI:10.1007/978-1-4939-9752-7_10.
- Wang R, Lu Y, Wang S. Comparative evaluation of 11 scoring functions for molecular docking. *J Med Chem*. 2003;46(12):2287-303. DOI:10.1021/jm0203783.
- Van Der Spoel D, Lindahl E, Hess B, Groenhof G, Mark AE, Berendsen HJC. GROMACS: fast, flexible, and free. *J Comput Chem*. 2005;26(16):1701-18. DOI: 10.1002/jcc.20291.
- Huang J, Mackerell AD. CHARMM36 all-atom additive protein force field: validation based on comparison to NMR data. *J Comput Chem*. 2013;34(25):2135-45. DOI:10.1002/jcc.23354.
- Zoete V, Cuendet MA, Grosdidier A, Michielin O. SwissParam: A fast force field generation tool for small organic molecules.

- J Comput Chem.* 2011;32(11):2359-68. DOI: 10.1002/jcc.21816.
36. Mark P, Nilsson L. Structure and Dynamics of the TIP3P, SPC, and SPC/E Water Models at 298 K. *J Phys Chem A.* 2001;105(43):9954-60. DOI: 10.1021/jp003020w.
 37. Bussi G, Donadio D, Parrinello M. Canonical sampling through velocity rescaling. *J Chem Phys.* 2007;126(1):014101. DOI: 10.1063/1.2408420.
 38. Darden T, York D, Pedersen L. Particle mesh Ewald: An N.log(N) method for Ewald sums in large systems. *J Chem Phys.* 1998;98(12):10089-92. DOI: 10.1063/1.464397.
 39. Jolliffe IT, Cadima J. Principal component analysis: a review and recent developments. *Philos Trans A Math Phys Eng Sci.* 2016;374(2065):20150202. DOI: 10.1098/rsta.2015.0202.
 40. Lever J, Krzywinski M, Altman N. Points of Significance: Principal component analysis. *Nat Methods.* 2017;14(7):641-2. DOI: 10.1038/nmeth.4346.
 41. Tavernelli I, Cotesta S, Di Iorio EE. Protein dynamics, thermal stability, and free-energy landscapes: A molecular dynamics investigation. *Biophys J.* 2003;85(4):2641. DOI:10.1016/s0006-3495(03)74687-6.
 42. Valdés-Tresanco MS, Valdés-Tresanco ME, Valiente PA, Moreno E. Gmx_MMPBSA: a new tool to perform end-state free energy calculations with GROMACS. *J Chem Theory Comput.* 2021;17(10):6281-91. DOI: 10.1021/acs.jctc.1c00645.
 43. Miller BR, McGee TD, Swails JM, Homeyer N, Gohlke H, Roitberg AE. MMPBSA.py: An efficient program for end-state free energy calculations. *J Chem Theory Comput.* 2012;8(9):3314-21. DOI: 10.1021/ct300418h.
 44. Meng XY, Zhang HX, Mezei M, Cui M. Molecular Docking: A powerful approach for structure-based drug discovery. *Curr Comput Aided Drug Des.* 2011;7(2):146-57. DOI: 10.2174/157340911795677602.
 45. Du X, Li Y, Xia YL, Ai SM, Liang J, Sang P, Ji XL, Liu SQ. Insights into protein-ligand interactions: Mechanisms, models, and methods. *Int J Mol Sci.* 2016;17(2):144. DOI: 10.3390/ijms17020144.
 46. Zheng X, Bauer P, Baumeister T, et al. Structure-based discovery of novel amide-containing nicotinamide phosphoribosyltransferase (NAMPT) inhibitors. *J Med Chem.* 2013;56(16):6413-33. DOI: 10.1021/jm4008664.
 47. Khan JA, Tao X, Tong L. Molecular basis for the inhibition of human NMPRTase, a novel target for anticancer agents. *Nat Struct Mol Biol.* 2006;13(7):582-8. DOI: 10.1038/nsmb1105.
 48. Arai M. Unified understanding of folding and binding mechanisms of globular and intrinsically disordered proteins. *Biophys Rev.* 2018;10(2):163. DOI: 10.1007/s12551-017-0346-7.
 49. Maisuradze GG, Liwo A, Scheraga HA. Principal component analysis for protein folding dynamics. *J Mol Biol.* 2009;385(1):312-29. DOI: 10.1016/j.jmb.2008.10.018.
 50. Altis A, Otten M, Nguyen PH, Hegger R, Stock G. Construction of the free energy landscape of biomolecules via dihedral angle principal component analysis. *J Chem Phys.* 2008;128(24):244902. DOI: 10.1063/1.2945165.
 51. Tavernelli I, Cotesta S, Di Iorio EE. Protein dynamics, thermal stability, and free-energy landscapes: a molecular dynamics investigation. *Biophys J.* 2003;85(4):2641-9. DOI: 10.1016/s0006-3495(03)74687-6.
 52. Yang LQ, Ji XL, Liu SQ. The free energy landscape of protein folding and dynamics: a global view. *J Biomol Struct Dyn.* 2013;31(9):982-92. DOI: 10.1080/07391102.2012.748536.

PEER-REVIEWED CERTIFICATION

During the review of this manuscript, a double-blind peer-review policy has been followed. The author(s) of this manuscript received review comments from a minimum of two peer-reviewers. Author(s) submitted revised manuscript as per the comments of the assigned reviewers. On the basis of revision(s) done by the author(s) and compliance to the Reviewers' comments on the manuscript, Editor(s) has approved the revised manuscript for final publication.